

# Nonsmooth modeling of distributed impacts in spatially discretized continuous structures using the Ivanov transformation

C. P. Vyasarayani\*, Surya Samukham and S. N. Khaderi  
Department of Mechanical and Aerospace Engineering  
Indian Institute of Technology Hyderabad  
Kandi, Sangareddy, 502285, Telangana, India

August 2, 2019

## Abstract

*This work deals with the modeling of nonsmooth impacting motions of a structure against a rigid distributed obstacle. Finite element methods can be used to discretize the structure, and this results in a system of ordinary differential equations (ODEs). When these ODEs are subjected to unilateral constraints and velocity jump conditions, one has to use an event detection algorithm to calculate the time of impact accurately. Event detection in the presence of multiple simultaneous impacts is a nontrivial and computationally demanding task. Ivanov (Ivanov, A., 1993. Analytical methods in the theory of vibro-impact systems. Journal of Applied Mathematics and Mechanics, 57(2), pp. 221-236.) proposed a nonsmooth transformation for a vibro-impacting multi-degree-of-freedom (MDOF) system subjected to only a single unilateral constraint. This transformation eliminates the unilateral constraints from the problem and, therefore, no event detection is required during numerical integration. This nonsmooth transformation leads to sign function nonlinearities in the equations of motion. However, they can be easily accounted during numerical integration. Ivanov used his transformation to make analytical calculations for the stability and bifurcations of vibro-impacting motions, but did not explore its application to simulating distributed collisions in discretized continuous structures. We adopt the Ivanov transformation to deal with multiple unilateral constraints in discretized continuous structures. The developed method is demonstrated by modeling the distributed collision of a string and a beam against a rigid surface. For validation, we compare our results with the penalty approach.*

---

\*Address all correspondence to this author. E-mail address: vcprakash@iith.ac.in

# 1 Introduction

In many engineering applications, structures are subjected to vibro-impacting motions [1, 2, 3]. Clearances in mechanical joints due to wear can lead to vibro-impacting motions in machine components. In some vibration-based energy harvesting applications, vibro-impacting motions are deliberately introduced to increase the bandwidth of the frequency response [4]. Some musical instruments of Indian origin, like the sitar and the tanpura, exploit vibro-impacting motions for tone generation [5]. In this work, we are interested in the problem of modeling the vibro-impacting motion of a continuous structure impacting a rigid distributed obstacle. When a continuous structure is spatially discretized using the finite element method, there are three ways the impacting motion can be simulated. The first method approximates the rigid obstacle as a foundation of springs with high stiffness and is known as the penalty approach [6]. Alternatively, one can use Lagrange multipliers to impose the contact constraints once the structure comes into contact with the obstacle. Complementarity conditions between Lagrange multipliers and gap functions are used to impose contact loss [7]. The Lagrange multiplier approach simulates the perfect sticking motion of the vibro-impacting systems [7]. Impacts can also be simulated using a coefficient of restitution (CoR) approach [6, 8]. Once contact is detected between the structure and the obstacle, the appropriate velocity jump conditions are imposed at the point of contact. In the Lagrange multiplier and CoR approaches, one has to solve an event detection problem to detect the time of impact accurately. Multiple simultaneous impacts are presenting when a structure impacts a distributed obstacle, and so the event detection problem becomes computationally expensive.

Within the framework of the CoR-based approach, Ivanov [9, 10] proposed a nonsmooth spatial transformation that automatically satisfies both unilateral constraints and velocity jump conditions at the point of contact. This approach eliminates the need for event detection. Ivanov proposed this method to study vibro-impacting motions of a multi-degree-of-freedom (MDOF) system, where the displacement of a single mass is constrained. The Ivanov transformation was successfully used to study the nonlinear dynamics of a single-degree-of-freedom (SDOF) vibro-impacting ship motion [11, 12]. In this work, we adopt the Ivanov transformation to account for the multiple unilateral constraints in a MDOF system. Overall, the main advantages of the Ivanov method are the following:

1. The nonsmooth nature of the contact problem is preserved, which is not the case with the penalty approach.
2. The equations in Ivanov's coordinates are non-stiff, in contrast to those in the penalty approach.
3. No event detection is necessary for simulating impacts, which is the most important benefit of Ivanov's approach as the problem of event detection is challenging in the case of large MDOF systems (like finite element models) subjected to distributed collisions.

The paper is organized as follows: In Sec. 2.1, we describe in detail how the Ivanov transformation works by modeling a point mass falling on a rigid obstacle. Using the example

of a vibro-impacting SDOF system, we compare the advantages of the Ivanov method over the penalty method in Sec. 2.2. The equations of motion for a nonlinear MDOF system in Ivanov's coordinates are derived in Sec 2.3. In Sec. 3, we apply the Ivanov transformation to simulate the motion of a string and beam impacting a distributed obstacle. The results are validated and compared with the penalty approach. Concluding remarks are presented in Sec. 4.

## 2 Mathematical modeling

In this section, using the example of a point mass bouncing on a rigid surface, we illustrate the idea behind the Ivanov transformation. Later, by using the example of a vibro-impacting oscillator, we demonstrate the advantages of modeling impact using Ivanov's method over the penalty approach. When simulating rigid collisions using a penalty approach, the penalty stiffness term is usually selected to be large, which results in stiff differential equations. Due to the stiff nature of the differential equations, one has to use a very small time step during numerical integration. However, in Ivanov's method, the obtained differential equations in the transformed coordinates are non-stiff. Unlike the penalty approach, Ivanov's method captures the nonsmooth behavior in velocity during impact precisely.

### 2.1 Point mass bouncing on a rigid surface

To illustrate the Ivanov transformation, we consider the problem of a point mass, under the influence of gravity, impacting a rigid surface (see Fig. 1). The equation of motion for this problem can be written as follows:

$$\ddot{p} = -g, \quad p \geq 0, \quad (1)$$

with initial conditions  $p(0) = \alpha_0$  and  $\dot{p}(0) = \beta_0$ . When the mass makes contact with the obstacle ( $p(t_c) = 0$ ) at time  $t_c$ , the following jump condition in velocity must be respected:

$$\dot{p}(t_c^+) = -R\dot{p}(t_c^-), \quad (2)$$

where,  $R$  is the coefficient of restitution. Equations (1) and (2) completely describe the motion of the mass. To apply the Ivanov transformation, we have to recast Eqs. (1) and (2) in state-space form. Introducing  $u = p$  and  $v = \dot{p}$ , we get

$$\begin{Bmatrix} \dot{u} \\ \dot{v} \end{Bmatrix} = \begin{bmatrix} 0 & 1 \\ 0 & 0 \end{bmatrix} \begin{Bmatrix} u \\ v \end{Bmatrix} + \begin{Bmatrix} 0 \\ -g \end{Bmatrix}, \quad u \geq 0 \quad (3)$$

and when  $u(t_c) = 0$ , we have

$$v(t_c^+) = -Rv(t_c^-). \quad (4)$$

Ivanov introduced the following nonsmooth transformation:

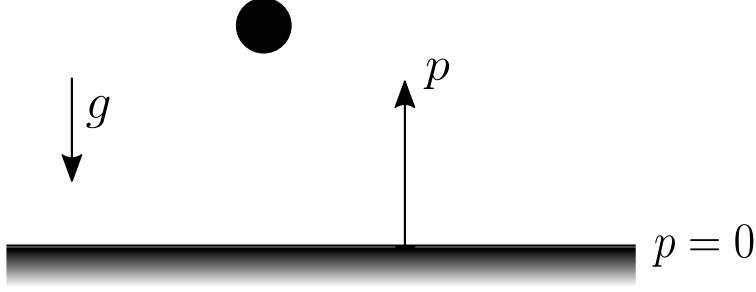


Figure 1: Schematic of a point mass falling on a rigid surface.

$$u = \eta \operatorname{sgn}(\eta) \quad (5)$$

$$v = \zeta (1 - k \operatorname{sgn}(\eta\zeta)) \operatorname{sgn}(\eta) \quad (6)$$

In Eq. (6),  $k = \frac{1-R}{1+R}$ . Equation (5) ensures that  $u \geq 0$  for all time. To understand the transformation given by Eq (6), we need to look at the phase-space of  $\eta - \zeta$ , as shown in Fig. 2(b); the actual phase-space (in  $u - v$ ) is shown in Fig. 2(a) for comparison. In the first and third quadrants of the  $\eta - \zeta$  plane, we have  $\operatorname{sgn}(\eta\zeta) > 0$ . In the second and fourth quadrants of the  $\eta - \zeta$  plane, we have  $\operatorname{sgn}(\eta\zeta) < 0$ . When a trajectory  $AB^-$  starting in phase-space  $\eta - \zeta$  from point  $A$  is about to cross  $\eta = 0$  at time  $t_B^-$  from the fourth to the third quadrant, from Eq. (6), we have:

$$v(t_B^-) = (1 + k) \zeta(t_B^-) \quad (7)$$

Immediately after the contact, at time  $t_B^+$ , we have:

$$v(t_B^+) = - (1 - k) \zeta(t_B^+) \quad (8)$$

Similarly, when the trajectory  $B^+C^-$  is about to cross  $\eta = 0$  at time  $t_C^-$  from the second to the first quadrant, we have:

$$v(t_C^-) = - (1 + k) \zeta(t_C^-) \quad (9)$$

After crossing  $\eta = 0$ , we have:

$$v(t_C^+) = (1 - k) \zeta(t_C^+) \quad (10)$$

It should be noted that both  $\eta$  and  $\zeta$  are continuous, so we have  $\zeta(t_B^-) = \zeta(t_B^+)$  and  $\zeta(t_C^-) = \zeta(t_C^+)$ , which results in the following expressions:

$$v(t_B^+) = - \left( \frac{1 - k}{1 + k} \right) v(t_B^-) = -Rv(t_B^-) \quad (11)$$

$$v(t_C^+) = - \left( \frac{1 - k}{1 + k} \right) v(t_C^-) = -Rv(t_C^-) \quad (12)$$

Therefore, it is clear that the nonsmooth transformation given by Eq. (6) automatically satisfies Eq. (4) at the event of impact. Due to the jump conditions (Eq. (11) and Eq. (12)) imposed on the velocity  $v$  at the time of impact, the trajectories in  $\eta - \zeta$  space that enter

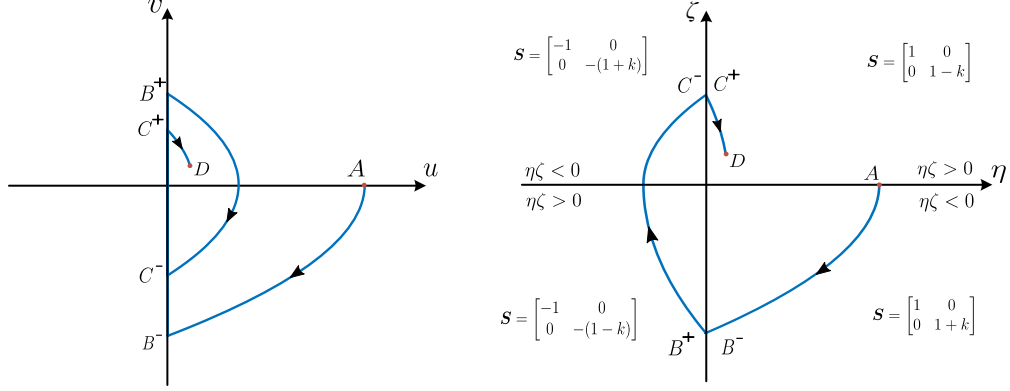


Figure 2: (a) Phase space in  $u$  and  $v$  coordinates. (b) Phase space in transformed  $\eta$  and  $\zeta$  coordinates.

the third quadrant from the fourth quadrant can only go to the first quadrant through the second quadrant. Equations (5) and (6) can be written as follows:

$$\begin{Bmatrix} u \\ v \end{Bmatrix} = \mathbf{S} \begin{Bmatrix} \eta \\ \zeta \end{Bmatrix} \quad (13)$$

The transformation matrix,  $\mathbf{S}$  in Eq. (13) is given by

$$\mathbf{S} = \begin{bmatrix} \text{sgn}(\eta) & 0 \\ 0 & (1 - k \text{sgn}(\eta\zeta)) \text{sgn}(\eta) \end{bmatrix} \quad (14)$$

The matrix,  $\mathbf{S}$  is constant in each quadrant of phase-space (see Fig. 2). Substituting Eq. (13) into Eq. (3), we get

$$\begin{Bmatrix} \dot{\eta} \\ \dot{\zeta} \end{Bmatrix} = \mathbf{S}^{-1} \begin{bmatrix} 0 & 1 \\ 0 & 0 \end{bmatrix} \mathbf{S} \begin{Bmatrix} \eta \\ \zeta \end{Bmatrix} + \mathbf{S}^{-1} \begin{Bmatrix} 0 \\ -g \end{Bmatrix} \quad (15)$$

The initial conditions for  $\eta$  and  $\zeta$  can be calculated as follows:

$$\begin{Bmatrix} \eta(0) \\ \zeta(0) \end{Bmatrix} = \mathbf{S}^{-1} \begin{Bmatrix} u(0) \\ v(0) \end{Bmatrix} \quad (16)$$

Equation (15) can be integrated numerically to obtain  $\eta$  and  $\zeta$ . Later, Eq. (13) can be used to calculate  $u$  and  $v$ . It should be noted that there are no constraints on Eq. (15) and its solutions are continuous functions of time. Figure 3(a) shows the displacement of the point mass in transformed coordinates ( $\eta$ , solid blue line) and physical coordinates ( $u$ , red dashed line). Similarly, Fig. 3(b) shows the velocity in transformed ( $\zeta$ , solid blue line) and physical ( $v$ , red dashed line) coordinates. Figure 3(c) shows the total energy of the point mass, and it can be seen that energy is lost at every collision. If we integrate Eq. (15) for a sufficiently long time, the energy will approach zero. Also, the frequency of solution,  $\eta$  continuously increases due to the chattering nature of the physical solution,  $u$ . If we use an adaptive time step integrator, the integrator automatically reduces the time steps to account for increasing frequency in the solution,  $\eta$ . For practical reasons, if the energy falls below a small threshold, we can assume that the point mass has reached equilibrium.

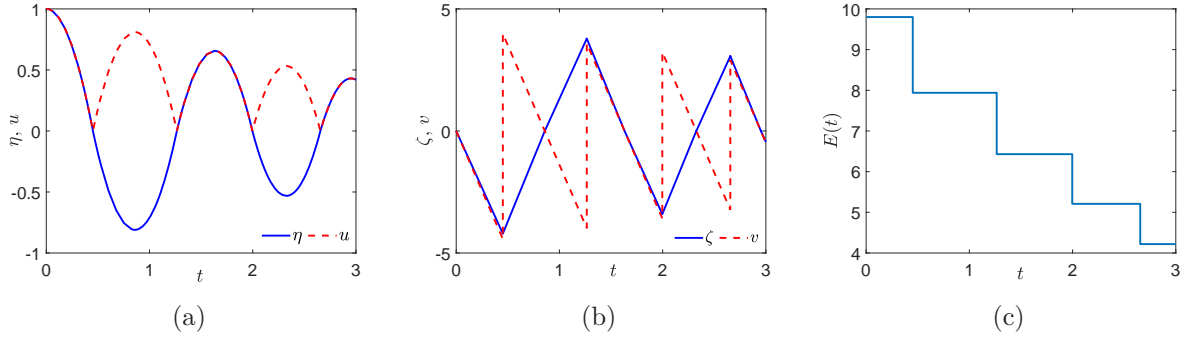


Figure 3: (a) Position of the point mass in physical ( $u$ ) and transformed coordinates ( $\eta$ ). (b) Velocity of the point mass in physical ( $v$ ) and transformed ( $\zeta$ ) coordinates. (c) Energy of the point mass over time. The results were obtained for  $u(0) = 1$ ,  $v(0) = 0$ ,  $g = 9.8$ , and  $R = 0.9$ .

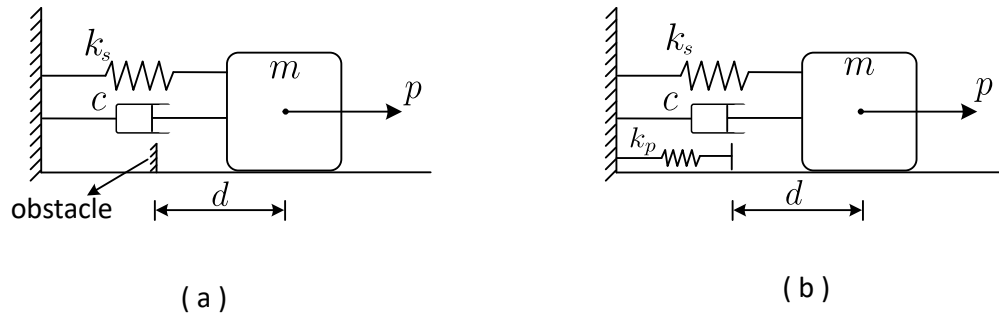


Figure 4: (a) Schematic of a spring-mass system with an obstacle. (b) Equivalent representation of the spring-mass system with the rigid obstacle replaced by a linear spring.

## 2.2 Single-degree-of-freedom vibro-impacting system

To demonstrate the advantage of modeling impact using Ivanov's method over a penalty approach, we consider the problem of a single-degree-of-freedom vibro-impacting system, as shown in Fig. 4(a). In the penalty approach, the rigid obstacle as shown in Fig. 4(a) is replaced with a high-stiffness ( $k_p$ ) linear spring (see Fig. 4(b)). For a large value of  $k_p$ , the spring behaves approximately like a rigid obstacle. In a penalty approach, we solve the following equation:

$$m\ddot{p} + c\dot{p} + (k_s + \mu k_p)p = 0 \quad (17)$$

In Eq. (17),  $\mu$  is defined as follows:

$$\mu = \begin{cases} 0 & p \geq 0 \\ 1 & p < 0 \end{cases} \quad (18)$$

From Eq. (17), we can see that the system has a time scale of  $\tau_1 = 2\pi\sqrt{\frac{m}{k_s}}$  when the mass is not in contact with the obstacle ( $\mu = 0$ ); when the mass is in contact with the obstacle ( $\mu = 1$ ), it has a time scale of  $\tau_2 = 2\pi\sqrt{\frac{m}{k_s+k_p}}$ . Having two separate time scales of very different magnitudes makes Eq. (17), a stiff differential equation. Therefore, when an explicit integrator is used to solve Eq. (17), one has to use a time step that is much smaller than  $\tau_2$  (the smallest time scale present in the solution) to obtain accurate results. The equation of motion of the vibro-impacting system, considering a perfectly rigid obstacle ( $R = 1$ ), can be written as follows:

$$m\ddot{p} + c\dot{p} + k_s p = 0, p \geq d \quad (19)$$

To apply Ivanov's method for solving the vibro-impact problem (Eq. (19)), we substitute  $u = p - d$  and  $v = \dot{p}$  in Eq. (19) to obtain:

$$\begin{Bmatrix} \dot{u} \\ \dot{v} \end{Bmatrix} = \begin{bmatrix} 0 & 1 \\ -k_s/m & -c/m \end{bmatrix} \begin{Bmatrix} u \\ v \end{Bmatrix} + \begin{Bmatrix} 0 \\ -k_s d/m \end{Bmatrix}, u \geq 0 \quad (20)$$

By following the same transformation as discussed for the point mass bouncing problem (see Eq. (5) and Eq. (6)), we can write the equations of motion of the vibro-impacting system with perfectly rigid impacts in Ivanov's coordinates as follows:

$$\begin{Bmatrix} \dot{\eta} \\ \dot{\zeta} \end{Bmatrix} = \mathbf{S}^{-1} \begin{bmatrix} 0 & 1 \\ -k_s/m & -c/m \end{bmatrix} \mathbf{S} \begin{Bmatrix} \eta \\ \zeta \end{Bmatrix} + \mathbf{S}^{-1} \begin{Bmatrix} 0 \\ -k_s d/m \end{Bmatrix} \quad (21)$$

See Eq. (14) for the definition of the matrix,  $\mathbf{S}$ . As pointed out earlier (see Fig. 2), the matrix  $\mathbf{S}$  is diagonal and a constant matrix in each quadrant of the phase-space. Further, the magnitude of the elements of  $\mathbf{S}$  are of the same order in all quadrants (see Fig. 2). Therefore, when an explicit integrator is used to solve Eq. (21), it does not appear as a stiff equation to the integrator.

We now demonstrate the advantage of the Ivanov method over the penalty method using a numerical test case. A reference solution  $p_r(t)$  is obtained by solving Eq. (17) using the “ode45” (adaptive time step) integrator in Matlab with relative and absolute tolerances of  $1 \times 10^{-8}$ . This reference solution  $p_r(t)$  is used for comparing the results from a fixed-time-step explicit integrator. Next, we solve the same problem (Eq. (17)) using a fixed-time-step fourth-order Runge–Kutta integrator with different time steps:  $\Delta t = 0.01\tau_2$ ,  $0.1\tau_2$ , and  $0.3\tau_2$ . The obtained numerical solution ( $p(t)$ ) from the penalty approach is shown in Fig. 5(a)-5(c). Also, the error,  $e(t) = p_r(t) - p(t)$ , between the reference solution and the obtained solution ( $p(t)$ ) is shown in Fig. 5(d)-5(f). It is clearly observed from these results that the error in the solution from the penalty approach increases as the time step of the integrator increases. From Fig. 5(c) and Fig. 5(f), we note that the solution obtained from the penalty approach with the time step of  $\Delta t = 0.3\tau_2$  is erroneous and does not match with the reference solution. Now, we solve the same problem using Ivanov’s method (Eq. (19)) using the same fixed-time-step, fourth-order Runge–Kutta integrator. The solution obtained from Ivanov’s method at different time steps ( $\Delta t = 1\tau_2$ ,  $100\tau_2$ , and  $1000\tau_2$ ) along with the reference solution is shown in Fig. 6(a)-6(c). The error,  $e(t) = p_r(t) - p(t)$ , in the solution obtained with Ivanov’s method when compared to the reference solution is shown in Fig. 6(d)-6(f). It can be observed that the solutions obtained from Ivanov’s method match closely with the reference solution to the order of  $10^{-1}$  even for a time step of  $1000\tau_2$ . Also, it is observed that the error in the solution obtained from Ivanov’s method with a time step of  $\Delta t = 1000\tau_2$ , which is less than the error in the solution obtained from the penalty approach with a time step of  $\Delta t = 0.1\tau_2$ .

In summary, in the penalty approach, to obtain an accurate solution of a vibro-impact system, the time step has to be chosen very small when compared to the fastest time scale in the problem ( $\Delta t \ll \tau_2$ ). However, by using Ivanov’s method, an accurate solution can be obtained with a much larger time step. For simulating a rigid collision, one has to use a large value for the penalty stiffness, which puts a hard restriction on the numerical time step of the integrator. However, in Ivanov’s approach, the nonsmooth transformation simulates the case of infinite penalty stiffness, but without making the equations stiff. Also, in the penalty approach, due to the finite penalty stiffness, the duration of contact is also finite, and when the simulation is done for a long time, these accumulated contact times will introduce a phase shift in the solution as compared to Ivanov’s method. This phase shift can be seen in Fig.5(f). Therefore, the comparison between the Ivanov and penalty methods will be valid only for small simulation times (few impacts).

### 2.3 Ivanov transformation for distributed impacts

Having demonstrated the applicability and advantage of the Ivanov transformation for an SDOF system, we now discuss its extension to MDOF systems where only some degrees of freedom are subjected to impact constraints. In many finite element models, when higher-order shape functions are used as basis functions, both slopes and displacements become degrees of freedom. However, impacts are generally defined for displacement coordinates. For example, if an Euler-Bernoulli beam is discretized using Hermite shape functions, one obtains both slopes and displacements as nodal degrees of freedom. When such a beam



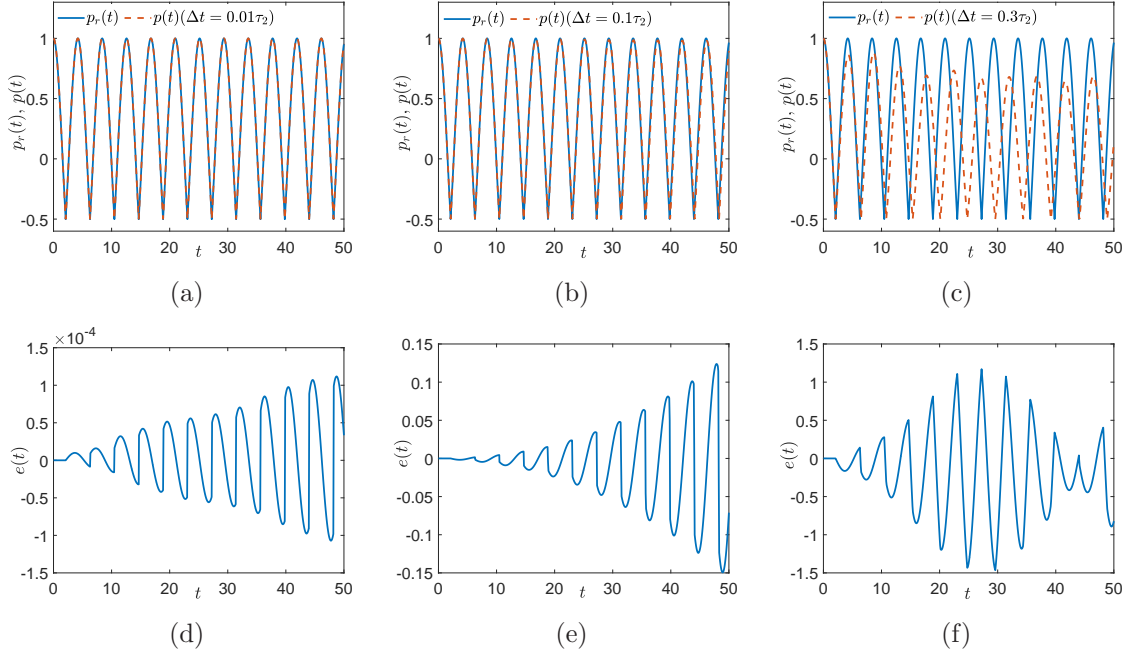


Figure 5: Solution of Eq. (17) obtained with the penalty method for different time steps: (a)  $\Delta t = 0.01\tau_2$ , (b)  $\Delta t = 0.1\tau_2$ , and (c)  $\Delta t = 0.3\tau_2$ . The error,  $e(t) = p_r(t) - p(t)$ , in the solution obtained from Ivanov's method for different time steps: (d)  $\Delta t = 0.01\tau_2$ , (e)  $\Delta t = 0.1\tau_2$ , and (f)  $\Delta t = 0.3\tau_2$ . The results were obtained using  $m = 1.0$ ,  $k_s = 1.0$ ,  $c = 0.0$ , and  $k_p = 1 \times 10^{10}$  in Eq. (17).

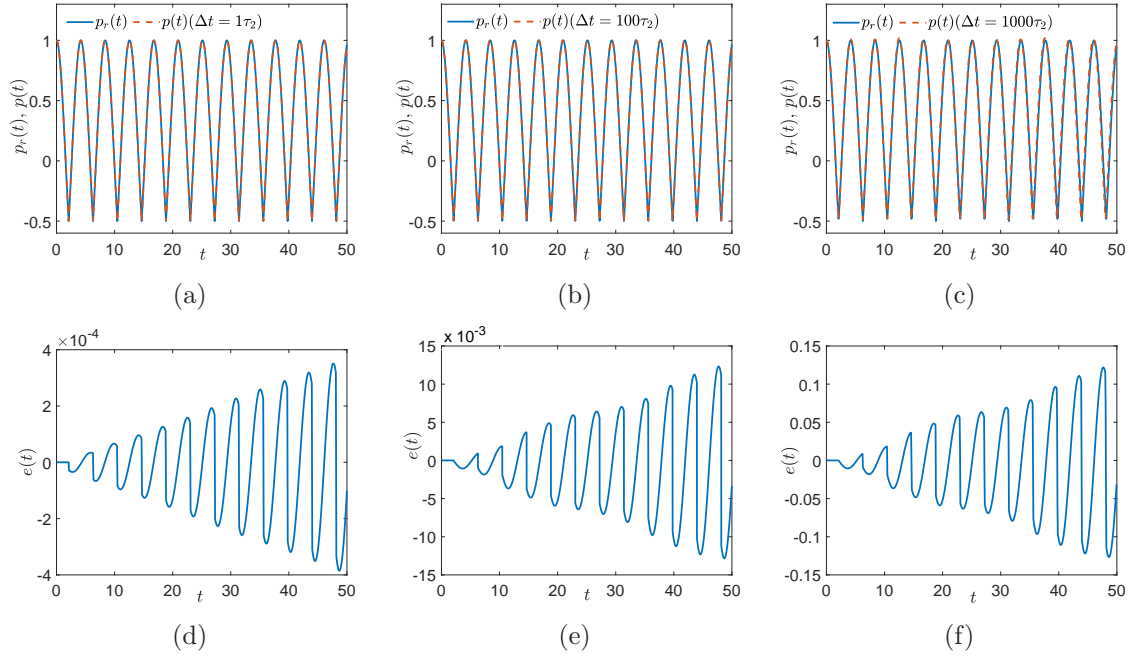


Figure 6: Solution of Eq. (19) obtained with Ivanov's method for different time steps: (a)  $\Delta t = \tau_2$ , (b)  $\Delta t = 100\tau_2$ , and (c)  $\Delta t = 1000\tau_2$ . The error,  $e(t) = p_r(t) - p(t)$ , in the solution obtained from Ivanov's method for different time steps: (d)  $\Delta t = \tau_2$ , (e)  $\Delta t = 100\tau_2$ , and (f)  $\Delta t = 1000\tau_2$ . The results were obtained using  $m = 1.0$ ,  $k_s = 1.0$ ,  $c = 0.0$ , and  $R = 1$  in Eq. (19).

makes contact with a rigid substrate, the displacements are constrained by impacts but not the rotations. Therefore, to develop the Ivanov transformation for the most general MDOF system, we consider the following coupled nonlinear model where some degrees of freedom ( $\mathbf{p}$ ) are subjected to impact while the others ( $\mathbf{q}$ ) are not subjected to any impact. The equations of motion for such a mechanical system can be written as follows:

$$\ddot{\mathbf{p}} = \mathbf{f}(\mathbf{p}, \dot{\mathbf{p}}, \mathbf{q}, \dot{\mathbf{q}}, t) \quad (22)$$

$$\ddot{\mathbf{q}} = \mathbf{g}(\mathbf{p}, \dot{\mathbf{p}}, \mathbf{q}, \dot{\mathbf{q}}, t) \quad (23)$$

subjected to initial conditions  $\mathbf{p}(\mathbf{0}) = \boldsymbol{\alpha}_0$ ,  $\dot{\mathbf{p}}(\mathbf{0}) = \boldsymbol{\beta}_0$ ,  $\mathbf{q}(\mathbf{0}) = \boldsymbol{\gamma}_0$ , and  $\dot{\mathbf{q}}(\mathbf{0}) = \boldsymbol{\nu}_0$ . In Eq. (22), the displacements coordinates  $\mathbf{p} = [p_1(t), p_2(t), \dots, p_m(t)]^T$  are subjected to impact constraints of the form:

$$p_i \geq d_i, \quad i = 1, 2, \dots, m \quad (24)$$

Once any of the above constraints becomes an equality constraint ( $p_i(t_c) = d_i$ ) at time  $t_c$ , a velocity jump condition is imposed as follows:

$$\dot{p}_i(t_c^+) = -R\dot{p}_i(t_c^-) \quad (25)$$

By defining  $\mathbf{d} = [d_1, d_2, \dots, d_m]^T$ , Eq. (24) can be compactly written as:

$$\mathbf{p} - \mathbf{d} \geq \mathbf{0} \quad (26)$$

It should be noted that the displacement coordinates  $\mathbf{q} = [q_1(t), q_2(t), \dots, q_n(t)]^T$  are not subjected to any impact constraints. By introducing the state variables  $\mathbf{u} = \mathbf{p} - \mathbf{d}$ ,  $\mathbf{v} = \dot{\mathbf{p}}$ ,  $\mathbf{r} = \mathbf{q}$ , and  $\mathbf{s} = \dot{\mathbf{q}}$ , Eq. (22) and Eq. (23) can be written as follows:

$$\dot{\mathbf{u}} = \mathbf{v} \quad (27)$$

$$\dot{\mathbf{v}} = \mathbf{f}(\mathbf{u} + \mathbf{d}, \mathbf{v}, \mathbf{r}, \mathbf{s}, t) \quad (28)$$

$$\dot{\mathbf{r}} = \mathbf{s} \quad (29)$$

$$\dot{\mathbf{s}} = \mathbf{g}(\mathbf{u} + \mathbf{d}, \mathbf{v}, \mathbf{r}, \mathbf{s}, t) \quad (30)$$

The impact constraint becomes  $\mathbf{u} \geq \mathbf{0}$ . Here  $\mathbf{u} = [u_1(t), u_2(t), \dots, u_m(t)]^T$ . Once any of the above constraints becomes an equality constraint ( $u_i(t_c) = 0$ ) at time  $t_c$ , a velocity jump condition is imposed as follows:

$$v_i(t_c^+) = -Rv_i(t_c^-) \quad (31)$$

To apply the Ivanov's method, the following transformation is introduced:

$$\mathbf{u} = \mathbf{T}\boldsymbol{\eta} \quad (32)$$

$$\mathbf{v} = \mathbf{W}\boldsymbol{\zeta} \quad (33)$$

The matrices  $\mathbf{T}$  and  $\mathbf{W}$  are defined as follows:

$$\mathbf{T} = \text{diag}(\text{sgn}(\boldsymbol{\eta})) \quad (34)$$

$$\mathbf{W} = \text{diag}((1 - k \text{sgn}(\boldsymbol{\eta} \circ \boldsymbol{\zeta})) \circ \text{sgn}(\boldsymbol{\eta})) \quad (35)$$

In Eq. (35), the symbol “o” represents the element-by-element multiplication (Hadamard product) of two vectors. Substituting Eq. (32) and Eq. (33) into Eqs. (27-30), we get

$$\dot{\boldsymbol{\eta}} = \mathbf{T}^{-1}\mathbf{W}\boldsymbol{\zeta} \quad (36)$$

$$\dot{\boldsymbol{\zeta}} = \mathbf{W}^{-1}\mathbf{f}(\mathbf{T}\boldsymbol{\eta} + \mathbf{d}, \mathbf{W}\boldsymbol{\zeta}, \mathbf{r}, \mathbf{s}, t) \quad (37)$$

$$\dot{\mathbf{r}} = \mathbf{s} \quad (38)$$

$$\dot{\mathbf{s}} = \mathbf{g}(\mathbf{T}\boldsymbol{\eta} + \mathbf{d}, \mathbf{W}\boldsymbol{\zeta}, \mathbf{r}, \mathbf{s}, t) \quad (39)$$

The initial conditions for Eqs. (36)-(39) are

$$\boldsymbol{\eta}(0) = \mathbf{T}^{-1}\mathbf{u}(0) = \mathbf{T}^{-1}(\mathbf{p}(0) - \mathbf{d}) = \mathbf{T}^{-1}(\boldsymbol{\alpha}_0 - \mathbf{d}) \quad (40)$$

$$\boldsymbol{\zeta}(0) = \mathbf{W}^{-1}\mathbf{v}(0) = \mathbf{W}^{-1}\dot{\mathbf{p}}(0) = \mathbf{W}^{-1}\boldsymbol{\beta}_0 \quad (41)$$

$$\mathbf{r}(0) = \mathbf{q}(0) = \boldsymbol{\gamma}_0 \quad (42)$$

$$\mathbf{s}(0) = \dot{\mathbf{q}}(0) = \boldsymbol{\nu}_0 \quad (43)$$

Solution of Eqs. (36)-(39) automatically satisfies all the constraints imposed on  $\mathbf{p}$  (Eq. 24) and  $\dot{\mathbf{p}}$  (Eq. (25)). Equations (36)-(39) are the closed form equations for a nonlinear MDOF system (where only some degrees of freedom are subjected to constraints) in Ivanov’s coordinates. Upon solving the system in Ivanov’s coordinates, the physical solution (displacements and velocities) can be reconstructed by using the inverse of the transformations given by Eqs. (32)-(33).

### 3 Results and discussion

We now validate the proposed approach by solving two problems: (1) the impact of a string on a distributed obstacle (see Fig. 7) and (2) the impact of a beam on a distributed obstacle. In our numerical studies, the tension and mass density of the string, as well as the flexural rigidity and mass density of the beam, are taken to be unity. The validation is performed by comparing our solution with that obtained using the penalty approach, where the obstacle is modeled as a foundation of unilateral linear springs with a spring constant of  $1 \times 10^8$  in the case of the string and  $1 \times 10^{20}$  in the case of the beam. All numerical simulations have been carried out in Matlab using the “ode45” built-in, adaptive-time-step numerical integrator with absolute and relative tolerances of  $1 \times 10^{-8}$ . The penalty stiffness for the string and the beam were selected to get a good match of response with Ivanov’s method. It should be noted that Ivanov’s method is a limiting case of the penalty approach (with infinite penalty stiffness) and it is to be expected that the results from these methods will match only for large values of penalty stiffness.

We now discuss the results for the string impact problem. The equations of motion of the string, in the absence of collisions, is obtained using the finite element method [13], using 250 nodes. The deflection of the string is linearly interpolated within each element using Lagrange shape functions. The elemental stiffness and lumped mass matrices are assembled to obtain the global lumped mass matrix ( $\mathbf{M}$ ) and global stiffness matrix ( $\mathbf{K}$ ). Then, the degrees

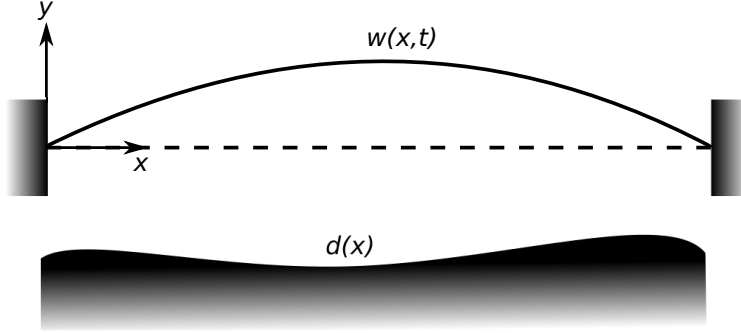


Figure 7: Schematic of a string with a distributed constraint.

of freedom corresponding to boundary conditions are eliminated, thereby obtaining, a 248 degree-of-freedom model for the string. We assume that the obstacle is located at a distance of  $-0.5$  from the string equilibrium. Therefore, we have  $d_i = -0.5, i = 1, 2, \dots, 248$ . The initial displacement condition is considered to be  $\sin(\pi x)$ , and the initial velocity condition is assumed to be zero. On following Ivanov's approach discussed in Sec. 2.1, the solution for the problem is obtained. It should be noted that all the degrees of freedom of the string are subjected to the impact constraint. Therefore, the coordinates  $\mathbf{q}$  will not appear in Eq. (22) and Eq. (23) does not exist.

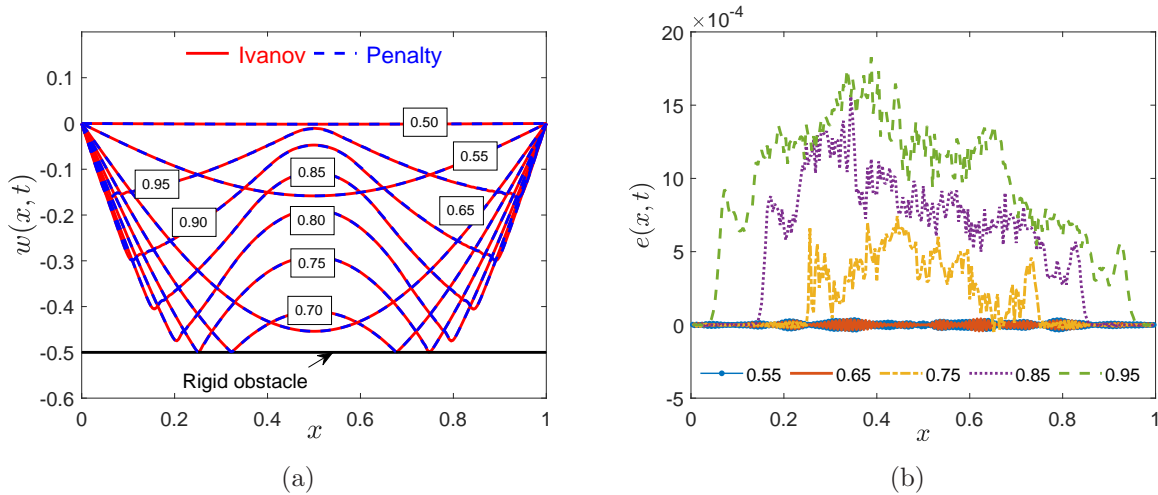


Figure 8: (a) Snapshots of the string motion impacting a flat obstacle obtained with the Ivanov transformation (red solid line) and penalty approach (blue dashed line). (b) Error in the string deflection between the solutions obtained with Ivanov's approach and the penalty method.

Figure 8 shows the shape of the string obtained from numerical simulations at different time instants for  $R = 1$  (CoR) and their corresponding errors (the difference between the Ivanov and penalty method solutions). It is clear from Fig. 8 that the results from the penalty and Ivanov transformation are nearly identical, with an error of order less than  $2 \times 10^{-3}$ . However, the unilateral constraints are exactly satisfied in Ivanov's approach; this is not

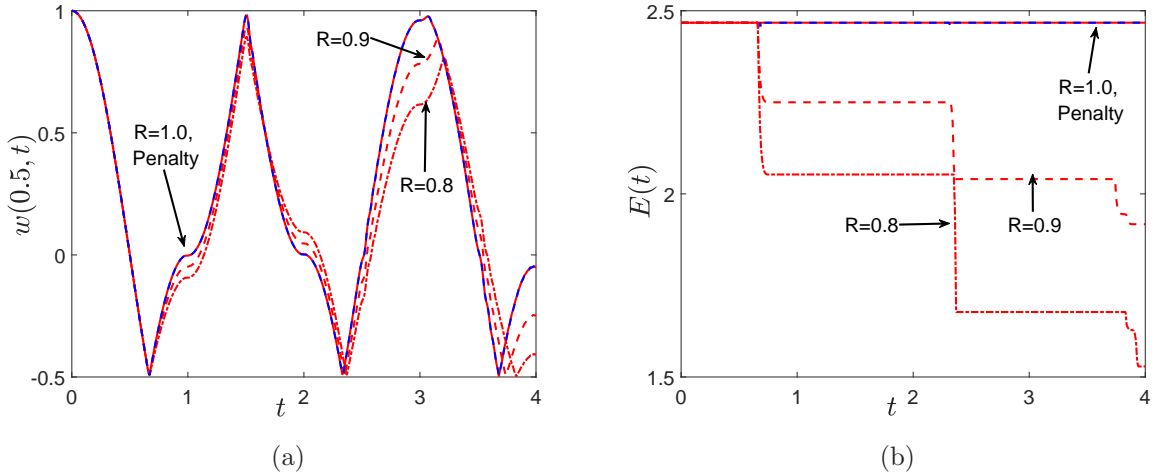


Figure 9: (a) Midpoint displacement and (b) energy of the string impacting a flat obstacle obtained with the Ivanov transformation for  $R = 1$  (solid red line),  $R = 0.9$  (red dashed line), and  $R = 0.8$  (red dotted line). The blue dashed lines show the results obtained using the penalty approach.

the case with the penalty approach. We can only compare results from Ivanov’s method for the case of  $R = 1$  with the penalty approach. This is because there are no models that relate  $R$  with contact dissipation in the penalty approach for discretized continuous systems. Figure 9(a) shows the midpoint deflection of the string for three values of  $R$ , and again we can see a good match between the penalty (blue dashed line) and Ivanov methods for  $R = 1$ . Figure 9(b) shows the total energy of the string (sum of kinetic and potential energy) for different values of  $R$ , and it is evident from the figure that energy is conserved for the case of  $R = 1$  in Ivanov’s method and the penalty approach (blue dashed line). For  $R < 1$ , energy is lost during every impact and, as expected, more energy is lost in the case of  $R = 0.8$  compared to  $R = 0.9$ .

As a second example, we consider the motion of a string impacting a sinusoidal obstacle  $d(x) = \sin(2\pi x)$ . The initial displacement condition for the string is assumed to be  $6 \sin(\pi x)$ , and the initial velocity is assumed to be zero. Figures 10 and 11 are similar to Fig. 8 and Fig. 9, except the results are presented for the case of a sinusoidal obstacle.

As a final example, we show the impact of a simply supported beam against a flat, rigid obstacle. The beam is given an initial displacement of  $\sin(\pi x)$  and slope of  $\pi \cos(\pi x)$ . The initial velocity is taken as zero. The flat obstacle is taken to be at  $d = -0.5$ . The above-mentioned problem is solved using Ivanov’s approach (discussed in Sec. 2.1) and the penalty method. The global mass (lumped) and global stiffness matrices are obtained by discretizing the beam using 50 two-noded Euler-Bernoulli finite elements. Due to the choice of Hermite polynomials as shape functions, at a given node the beam has both displacements  $\mathbf{p}$  and slopes  $\mathbf{q}$  as degrees of freedom. The obstacle restricts the motion of the displacements but not the slopes; thus, not all degrees of freedom are subjected to impact constraints (see Eq. (22) and Eq. (23)).

The snapshots of the beam at various time instances, obtained using the proposed

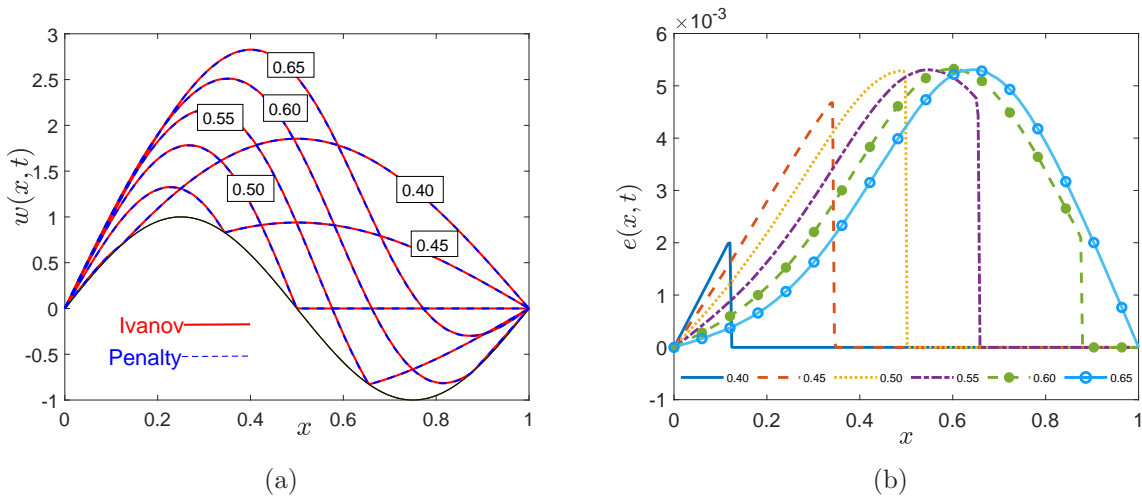


Figure 10: (a) Snapshots of the string motion impacting a sinusoidal obstacle obtained with the Ivanov transformation (solid red line) and the penalty approach (blue dashed line). (b) Error in the string deflection between the solutions obtained from Ivanov’s approach and the penalty method.

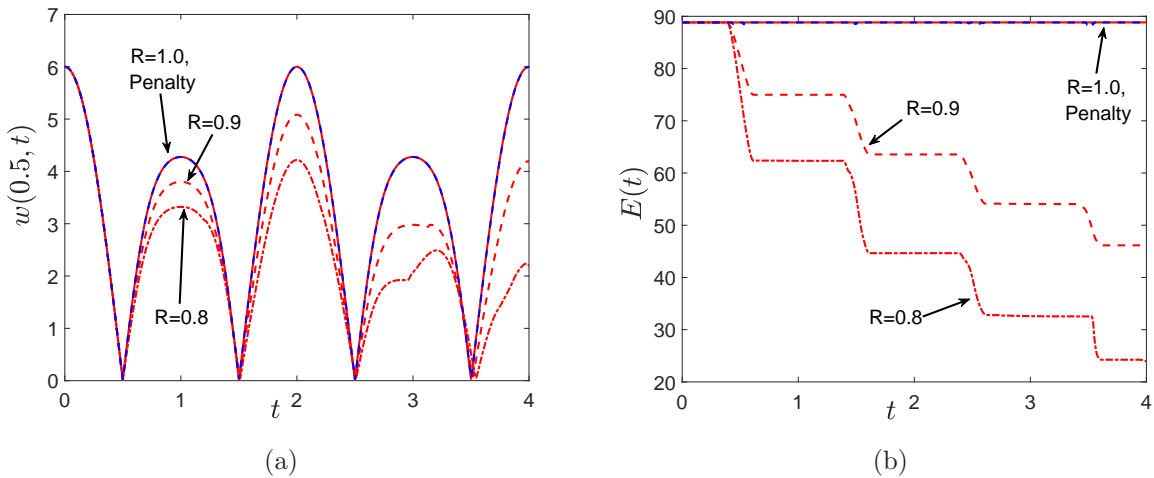


Figure 11: (a) Midpoint displacement and (b) energy of the string impacting a sinusoidal obstacle obtained with the Ivanov transformation for  $R = 1$  (solid red line),  $R = 0.9$  (red dashed line), and  $R = 0.8$  (red dotted line). The blue dashed lines show the results obtained using the penalty approach.

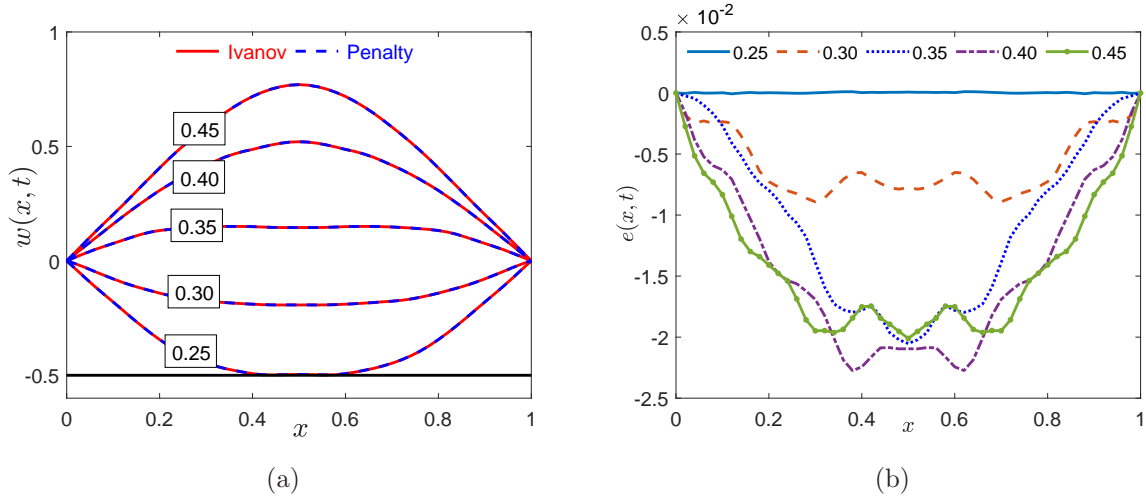


Figure 12: (a) Snapshots of the beam motion impacting a flat obstacle obtained with the Ivanov transformation (solid red line) and the penalty approach (blue dashed line) at different times. (b) Difference in the beam deflection between the solutions obtained from the Ivanov and penalty methods.

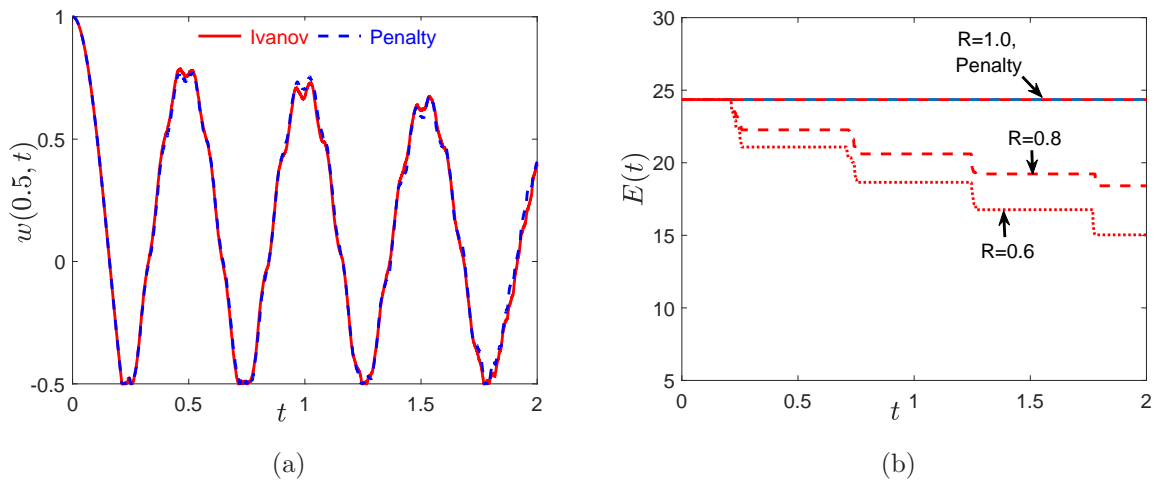


Figure 13: (a) Midpoint displacement and (b) energy of the beam impacting a flat obstacle obtained with the Ivanov transformation for  $R = 1$  (solid red line),  $R = 0.8$  (red dashed line), and  $R = 0.6$  (red dotted line). The blue dashed lines show the results obtained using the penalty approach.



method, are shown in Fig. 12(a) for  $R = 1$ . The error between the corresponding solutions obtained using Ivanov’s approach and the penalty method at these times are shown in Fig. 12(b). Results from Fig. 12, show that the solutions obtained using Ivanov’s transformation are in good agreement with those obtained using the penalty method. The deflection of the center of the beam and change in total energy with respect to time are plotted in Figs. 13(a)-(b), respectively. As expected, it is seen that the trajectory of the midpoint of the beam matches very well with the penalty method and the total energy of the beam decreases with each impact for  $R < 1$ . Even though we have reported results for a string and a beam, the approach can be used to simulate impacts in membranes or plate structures as well. Extension of this transformation to nonlinear MDOF models is also straightforward. It is clear from the above examples that the Ivanov transformation can successfully simulate vibro-impacting motions of discretized continuous structures with distributed contacts.

## 4 Conclusions

In this paper, we have adopted Ivanov’s transformation to simulate nonsmooth distributed impacts in spatially discretized continuous structures. A closed-form expression for nonlinear MDOF systems in Ivanov’s transformed coordinates is reported. The transformed differential equations are without any constraints and automatically satisfy the unilateral and velocity jump conditions at impact. The technique was validated by solving four model problems and comparing their solutions with those obtained using the penalty method. The equations of motion obtained from Ivanov’s method are not stiff, in contrast to those obtained from the penalty method. Therefore, a larger time step-size can be used during numerical integration of the equations of motion obtained from Ivanov’s method. The event detection problem for large MDOF systems in the presence of multiple impact constraints is a difficult and challenging task, and is completely eliminated by application of Ivanov’s method.

## Acknowledgments

CPV gratefully acknowledges the Department of Science and Technology for funding this research through Inspire fellowship (DST/INSPIRE/04/2014/000972).

## 5 Appendix

In this section, we have given the explicit equations of motion in Ivanov coordinates for the beam/string problem and its energy expressions.

### 5.1 Ivanov transformation for string/beam

In order to explain the procedure of applying Ivanov’s transformation to a finite element system with higher-order shape functions, a simply-supported beam is considered. Upon

applying the boundary conditions, the equations of motion for the resulting system are written in matrix form as:

$$\mathbf{M}\ddot{\mathbf{y}} + \mathbf{K}\mathbf{y} = \mathbf{0}, \quad (44)$$

where  $\mathbf{M}$  and  $\mathbf{K}$  are mass matrix and stiffness matrix, respectively, and  $\mathbf{y} = [\mathbf{p} \ \mathbf{q}]^T$  is the vector of unknowns. Here,  $\mathbf{p}$  and  $\mathbf{q}$  are the displacement vectors and slope vectors (which are absent in the case of a string), respectively. Equation (44) can be re-written as:

$$\ddot{\mathbf{y}} = \mathbf{A}\mathbf{y} \quad (45)$$

Here,  $\mathbf{A} = -\mathbf{M}^{-1}\mathbf{K}$ . By defining the variables  $\mathbf{u} = \mathbf{p} - \mathbf{d}$ ,  $\mathbf{v} = \dot{\mathbf{p}}$ ,  $\mathbf{r} = \mathbf{q}$  and  $\mathbf{s} = \dot{\mathbf{q}}$  (Eq. (27)-(30)), Eq. (45) can be written as:

$$\begin{Bmatrix} \dot{\mathbf{v}} \\ \dot{\mathbf{s}} \end{Bmatrix} = \begin{bmatrix} \mathbf{A}_{11} & \mathbf{A}_{12} \\ \mathbf{A}_{21} & \mathbf{A}_{22} \end{bmatrix} \begin{Bmatrix} \mathbf{u} \\ \mathbf{r} \end{Bmatrix} + \begin{bmatrix} \mathbf{A}_{11} & \mathbf{A}_{12} \\ \mathbf{A}_{21} & \mathbf{A}_{22} \end{bmatrix} \begin{Bmatrix} \mathbf{d} \\ \mathbf{0} \end{Bmatrix}, \quad (46)$$

where the matrices  $\mathbf{A}_{11}$ ,  $\mathbf{A}_{12}$ ,  $\mathbf{A}_{21}$  and  $\mathbf{A}_{22}$  contain the elements of matrix  $\mathbf{A}$  that correspond to the vectors  $\mathbf{u}$  and  $\mathbf{r}$ . From Eq. (46),  $\dot{\mathbf{v}}$  and  $\dot{\mathbf{s}}$  can be written as:

$$\dot{\mathbf{v}} = \mathbf{A}_{11}\mathbf{u} + \mathbf{A}_{12}\mathbf{r} + \mathbf{A}_{11}\mathbf{d} \quad (47)$$

$$\dot{\mathbf{s}} = \mathbf{A}_{21}\mathbf{u} + \mathbf{A}_{22}\mathbf{r} + \mathbf{A}_{21}\mathbf{d} \quad (48)$$

From the transformation  $\mathbf{u} = \mathbf{T}\boldsymbol{\eta}$  and  $\mathbf{v} = \mathbf{W}\boldsymbol{\zeta}$  (Eq. (32)-(33)), (where the matrices  $\mathbf{T}$  and  $\mathbf{W}$  are given in Eqs. (34)-(35)), Eqs. (47)-(48) become:

$$\dot{\boldsymbol{\eta}} = \mathbf{T}^{-1}\mathbf{W}\boldsymbol{\zeta} \quad (49)$$

$$\dot{\boldsymbol{\zeta}} = \mathbf{W}^{-1}\bar{\mathbf{A}}_{11}\mathbf{T}\boldsymbol{\eta} + \mathbf{W}^{-1}\bar{\mathbf{A}}_{12}\mathbf{r} + \mathbf{W}^{-1}\bar{\mathbf{A}}_{11}\mathbf{d} \quad (50)$$

$$\dot{\mathbf{r}} = \mathbf{I}\mathbf{s} \quad (51)$$

$$\dot{\mathbf{s}} = \bar{\mathbf{A}}_{21}\mathbf{T}\boldsymbol{\eta} + \bar{\mathbf{A}}_{22}\mathbf{r} + \bar{\mathbf{A}}_{21}\mathbf{d} \quad (52)$$

Here,  $\mathbf{I}$  is the identity matrix. By integrating the system of differential equations given by Eqs. (49)-(52), with the initial conditions mentioned in Eqs. (36)-(39), and transforming the obtained solution into the physical coordinates using Eqs. (32)-(33), the solution for Eq. (44) will be obtained.

## 5.2 Energy expression

The kinetic and potential energy of a continuous system are determined from the following expressions:

$$KE(t) = \frac{1}{2}\dot{\mathbf{y}}^T(t)\mathbf{M}\dot{\mathbf{y}}(t) \quad (53)$$

$$PE(t) = \frac{1}{2}\mathbf{y}^T(t)\mathbf{K}\mathbf{y}(t) \quad (54)$$

Here,  $\mathbf{M}$  and  $\mathbf{K}$  are the global mass matrix and global stiffness matrix of the structure, respectively.  $\mathbf{y}(t)$  and  $\dot{\mathbf{y}}(t)$  are the displacement and velocity vectors, respectively, at time  $t$ . Now, the total energy of the system,  $E(t)$ , is given as the sum of the kinetic energy ( $KE(t)$ ) and the potential energy ( $PE(t)$ ) at any instant of time.

## References

- [1] Babitsky, V. I., 1998. *Theory of vibro-impact systems and applications*. Berlin, Germany: Springer-Verlag.
- [2] Ibrahim, R. A., 2009. *Vibro-impact dynamics: modeling, mapping and applications*. Berlin, Heidelberg: Springer-Verlag.
- [3] Ibrahim, R. A., 2014. “Recent advances in vibro-impact dynamics and collision of ocean vessels”. *Journal of Sound and Vibration*, **333**(23), pp. 5900–5916.
- [4] Vijayan, K., Friswell, M., Khodaparast, H. H., and Adhikari, S., 2015. “Non-linear energy harvesting from coupled impacting beams”. *International Journal of Mechanical Sciences*, **96**, pp. 101–109.
- [5] Chatziioannou, V., and van Walstijn, M., 2015. “Energy conserving schemes for the simulation of musical instrument contact dynamics”. *Journal of Sound and Vibration*, **339**, pp. 262–279.
- [6] Gilardi, G., and Sharf, I., 2002. “Literature survey of contact dynamics modelling”. *Mechanism and Machine Theory*, **37**(10), pp. 1213–1239.
- [7] Wagg, D., 2005. “Periodic sticking motion in a two-degree-of-freedom impact oscillator”. *International Journal of Non-Linear Mechanics*, **40**(8), pp. 1076–1087.
- [8] Liakou, A., Denoël, V., and Detournay, E., 2016. “Fast in-plane dynamics of a beam with unilateral constraints”. *Journal of Engineering Mechanics*, **143**(2), p. 04016116.
- [9] Ivanov, A., 1993. “Analytical methods in the theory of vibro-impact systems”. *Journal of Applied Mathematics and Mechanics*, **57**(2), pp. 221–236.
- [10] Ivanov, A., 1994. “Impact oscillations: linear theory of stability and bifurcations”. *Journal of Sound and Vibration*, **178**(3), pp. 361–378.
- [11] Grace, I. M., Ibrahim, R. A., and Pilipchuk, V. N., 2011. “Inelastic impact dynamics of ships with one-sided barriers. Part I: analytical and numerical investigations”. *Nonlinear Dynamics*, **66**(4), pp. 589–607.
- [12] Grace, I. M., Ibrahim, R. A., and Pilipchuk, V. N., 2011. “Inelastic impact dynamics of ships with one-sided barriers. Part II: experimental validation”. *Nonlinear Dynamics*, **66**(4), pp. 609–623.
- [13] Zienkiewicz, O. C., and Taylor, R. L., 1977. *The finite element method*, Vol. 36. McGraw-Hill, London.